The imprint of the interaction between dark sectors in large scale cosmic microwave background anisotropies

Jian-Hua He[1], Bin Wang[1*], Pengjie Zhang[2]

[1] *Department of Physics, Fudan University, 200433 Shanghai, China and*

[2] *Key Laboratory for Research in Galaxies and Cosmology,*

Shanghai Astronomical Observatory, Nandan Road 80, Shanghai, 200030, China

Abstract

Dark energy interacting with dark matter is a promising model to solve the cosmic coincidence problem. We study the signature of such interaction on large scale cosmic microwave background (CMB) temperature anisotropies. Based on the detail analysis in perturbation equations of dark energy and dark matter when they are in interaction, we find that the large scale CMB, especially the late Integrated Sachs Wolfe effect, is a useful tool to measure the coupling between dark sectors. We also discuss the possibility to detect the coupling by cross-correlating CMB maps with tracers of the large scale structure. We finally perform the global fitting to constrain the coupling by using the CMB power spectrum data together with other observational data. We find that in the 1σ range, the constrained coupling between dark sectors can solve the coincidence problem.

PACS numbers: 98.80.Cq, 98.80.-k

* wangb@fudan.edu.cn

I. INTRODUCTION

Advances in cosmological observations have presented us a concordance picture that our present universe is accelerating and the dominant mass-energy components for the evolution of the universe in the standard model are non-baryonic cold dark matter (DM) and dark energy field (DE)[1, 2, 3]. The DE is identified as the engine for the accelerated expansion. The leading interpretation of such DE is a cosmological constant with equation of state (EoS) $w = -1$. While the cosmological constant is consistent with the observational data, at the fundamental level it fails to be convincing: the vacuum energy density falls below the value predicted by any sensible quantum field theory by many orders of magnitude, and it unavoidably leads to the coincidence problem, i.e., "why are the vacuum and matter energy densities of precisely the same order today?". More sophisticated models have been proposed to replace the cosmological constant by a dynamical dark energy in the conjectures relating the DE either to a scalar field called quintessence with $w > -1$, or to an exotic field called phantom with $w < -1$. However, there is no clear winner in sight to explain the nature of DE at the moment.

Most available discussions on the DE were in the minimal picture which assumed that DE does not feel any significant interactions from DM. Although this picture is consistent with current observations, considering that DE and DM account for significant fractions of the content of the Universe, it is still natural, in the framework of field theory, to consider their interaction. The possibility that DE and DM can interact with each other has been widely discussed recently[4]-[25]. It has been shown that the coupling between DE and DM can provide a mechanism to alleviate the coincidence problem [4, 5, 7, 8]. Furthermore, it was suggested that the dynamical equilibrium of collapsed structures such as clusters would get modification due to the coupling between DE and DM [13, 18]. The influences on the growth of cosmic structure due to the coupling between dark sectors were also shown in [25, 26]. Observational signatures on the dark sectors' mutual interaction have been found in the probes of the cosmic expansion history by using the SNIa, BAO and CMB shift data etc [14, 19, 20]. In addition, it has been argued that an appropriate interaction between DE and DM can influence the perturbation dynamics and affect the lowest multipoles of the CMB power spectrum [9, 10]. Recently there has been some concern about the stability of the perturbations if DE and DM interact [15]. However, it was proved in [16] that the stability of the curvature perturbation depends on the types of coupling between dark sectors and the EoS of DE. Based on the result in [16], we are in a position to carry out the global fitting to probe the interaction between dark sectors by using the CMB power spectrum data together with other observational data.

Recently the WMAP data showed the deficit of large scale power in the temperature map, in particular in the CMB quadrupole. The significant contribution to the fluctuations on these scales is the late Integrated Sachs Wolfe (ISW)

effect which is induced by the passage of CMB photons through the time evolving gravitational potential when the universe enters a rapid expansion phase once DE dominates. The late ISW effect has the unique ability to probe the "size" of DE. Much effort has been put into determining the EoS and the speed of sound of DE [27, 28]. Whether the late ISW can give insight into the coupling between dark sectors is an interesting question. In this paper we are going to discuss this problem in detail. We will further employ the CMB data from ground based and satellite observations together with SNIa and SDSS data to constrain the coupling between dark sectors.

The organization of the paper is as follows: in the following section we will review the general formalism of the perturbation theory in the presence of the interaction between DE and DM. In Sec.III we will discuss the large scale cosmic microwave anisotropies and its imprint on the "size" of DE, especially the coupling between dark sectors. In Sec.IV, we will present the global fitting result by using CMB data together with SNIa and SDSS data and we will discuss the alleviation of the coincidence problem when DE interacts with DM. We will present our conclusions and discussions in the end.

II. PERTURBATION THEORY WHEN DE INTERACTS WITH DM

In this section we will go over the perturbation theory when DE interacts with DM. The detailed descriptions can be found in [16, 25].

The perturbed metric at first order is of the form

$$ds^2 = a^2[-(1+2\psi)d\tau^2 + 2\partial_i B d\tau dx^i + (1+2\phi)\delta_{ij}dx^i dx^j + D_{ij}E dx^i dx^j], \tag{1}$$

where ψ, B, ϕ, E represent the scalar metric perturbations, a is the cosmic scale factor and

$$D_{ij} = (\partial_i\partial_j - \frac{1}{3}\delta_{ij}\nabla^2). \tag{2}$$

We work with general stress-energy tensor

$$T^{\mu\nu} = \rho U^\mu U^\nu + p(g^{\mu\nu} + U^\mu U^\nu), \tag{3}$$

for a two-component system consisting of DE and DM. Each energy-mementum tensor satisfies the conservation law

$$\nabla_\mu T^{\mu\nu}_{(\lambda)} = Q^\nu_{(\lambda)}, \tag{4}$$

where $Q^\nu_{(\lambda)}$ denotes the interaction between different components and λ denotes either the DM or the DE sector.

In the Fourier space the perturbed energy-momentum tensor reads [25]

$$\delta'_\lambda + 3\mathcal{H}(\frac{\delta p_\lambda}{\delta\rho_\lambda} - w_\lambda)\delta_\lambda = -(1+w_\lambda)kv_\lambda - 3(1+w_\lambda)\phi' + (2\psi - \delta_\lambda)\frac{a^2Q^0_\lambda}{\rho_\lambda} + \frac{a^2\delta Q^0_\lambda}{\rho_\lambda}$$

$$(v_\lambda + B)' + \mathcal{H}(1-3w_\lambda)(v_\lambda + B) = \frac{k}{1+w_\lambda}\frac{\delta p_\lambda}{\delta\rho_\lambda}\delta_\lambda - \frac{w'_\lambda}{1+w_\lambda}(v_\lambda + B) + k\psi - \frac{a^2Q^0_\lambda}{\rho_\lambda}v_\lambda - \frac{w_\lambda a^2Q^0_\lambda}{(1+w_\lambda)\rho_\lambda}B + \frac{a^2\delta Q_{p\lambda}}{(1+w_\lambda)\rho_\lambda}. \quad (5)$$

Constructing the gauge invariant quantities[25]

$$\begin{aligned}
\Psi &= \psi - \frac{1}{k}\mathcal{H}(B + \frac{E'}{2k}) - \frac{1}{k}(B' + \frac{E''}{2k}) \\
\Phi &= \phi + \frac{1}{6}E - \frac{1}{k}\mathcal{H}(B + \frac{E'}{2k}) \\
Q^{0I}_\lambda &= \delta Q^0_\lambda - \frac{Q^{0'}_\lambda}{\mathcal{H}}(\phi + \frac{E}{6}) + Q^0_\lambda\left[\frac{1}{\mathcal{H}}(\phi + \frac{E}{6})\right]' \\
\delta Q^I_{p\lambda} &= \delta Q_{p\lambda} - Q^0_\lambda\frac{E'}{2k} \\
D_{g\lambda} &= \delta_\lambda - \frac{\rho'_\lambda}{\rho_\lambda\mathcal{H}}\left(\phi + \frac{E}{6}\right) \\
V_\lambda &= v_\lambda - \frac{E'}{2k},
\end{aligned} \quad (6)$$

we obtain the gauge invariant linear perturbation equations for dark sectors. For DM it reads,

$$\begin{aligned}
&D'_{gc} + \left\{\left(\frac{a^2Q^0_c}{\rho_c\mathcal{H}}\right)' + \frac{\rho'_c}{\rho_c\mathcal{H}}\frac{a^2Q^0_c}{\rho_c}\right\}\Phi + \frac{a^2Q^0_c}{\rho_c}D_{gc} + \frac{a^2Q^0_c}{\rho_c\mathcal{H}}\Phi' \\
&= -kV_c + 2\Psi\frac{a^2Q^0_c}{\rho_c} + \frac{a^2\delta Q^{0I}_c}{\rho_c} + \frac{a^2Q^{0'}_c}{\rho_c\mathcal{H}}\Phi - \frac{a^2Q^0_c}{\rho_c}\left(\frac{\Phi}{\mathcal{H}}\right)' \\
&V'_c + \mathcal{H}V_c = k\Psi - \frac{a^2Q^0_c}{\rho_c}V_c + \frac{a^2\delta Q^I_{pc}}{\rho_c}
\end{aligned} \quad (7)$$

For DE, we have

$$\begin{aligned}
&D'_{gd} + \left\{\left(\frac{a^2Q^0_d}{\rho_d\mathcal{H}}\right)' - 3w' + 3(C_e^2 - w)\frac{\rho'_d}{\rho_d} + \frac{\rho'_d}{\rho_d\mathcal{H}}\frac{a^2Q^0_d}{\rho_d}\right\}\Phi + \left\{3\mathcal{H}(C_e^2 - w) + \frac{a^2Q^0_d}{\rho_d}\right\}D_{gd} + \frac{a^2Q^0_d}{\rho_d\mathcal{H}}\Phi' \\
&= -(1+w)kV_d + 3\mathcal{H}(C_e^2 - C_a^2)\frac{\rho'_d}{\rho_d}\frac{V_d}{k} + 2\Psi\frac{a^2Q^0_d}{\rho_d} + \frac{a^2\delta Q^{0I}_d}{\rho_d} + \frac{a^2Q^{0'}_d}{\rho_d\mathcal{H}}\Phi - \frac{a^2Q^0_d}{\rho_d}\left(\frac{\Phi}{\mathcal{H}}\right)' \\
&V'_d + \mathcal{H}(1-3w)V_d = \frac{kC_e^2}{1+w}D_{gd} + \frac{kC_e^2}{1+w}\frac{\rho'_d}{\rho_d\mathcal{H}}\Phi - (C_e^2 - C_a^2)\frac{V_d}{1+w}\frac{\rho'_d}{\rho_d} - \frac{w'}{1+w}V_d + k\Psi - \frac{a^2Q^0_d}{\rho_d}V_d + \frac{a^2\delta Q^I_{pd}}{\rho_d}
\end{aligned} \quad (8)$$

where we have employed

$$\frac{\delta p_d}{\rho_d} = C_e^2\delta_d - (C_e^2 - C_a^2)\frac{\rho'_d}{\rho_d}\frac{v_d + B}{k} \quad (9)$$

where C_e^2 is the effective sound speed of DE at the rest frame, C_a^2 is the adiabatic sound speed.

To alleviate the singular behavior caused by w crossing -1, we substitute V_λ into U_λ in the above equations where

$$U_\lambda = (1+w)V_\lambda. \quad (10)$$

Thus we can rewrite eq(7) and eq(8) into,

$$
\begin{aligned}
&D'_{gc}+\left\{\left(\frac{a^2Q^0_c}{\rho_c\mathcal{H}}\right)'+\frac{\rho'_c}{\rho_c\mathcal{H}}\frac{a^2Q^0_c}{\rho_c}\right\}\Phi+\frac{a^2Q^0_c}{\rho_c}D_{gc}+\frac{a^2Q^0_c}{\rho_c\mathcal{H}}\Phi'\\
&=-kU_c+2\Psi\frac{a^2Q^0_c}{\rho_c}+\frac{a^2\delta Q^{0I}_c}{\rho_c}+\frac{a^2Q^{0'}_c}{\rho_c\mathcal{H}}\Phi-\frac{a^2Q^0_c}{\rho_c}\left(\frac{\Phi}{\mathcal{H}}\right)'\\
&U'_c+\mathcal{H}U_c=k\Psi-\frac{a^2Q^0_c}{\rho_c}U_c+\frac{a^2\delta Q^I_{pc}}{\rho_c}
\end{aligned}
\tag{11}
$$

$$
\begin{aligned}
&D'_{gd}+\left\{\left(\frac{a^2Q^0_d}{\rho_d\mathcal{H}}\right)'-3w'+3(C_e^2-w)\frac{\rho'_d}{\rho_d}+\frac{\rho'_d}{\rho_d\mathcal{H}}\frac{a^2Q^0_d}{\rho_d}\right\}\Phi+\left\{3\mathcal{H}(C_e^2-w)+\frac{a^2Q^0_d}{\rho_d}\right\}D_{gd}+\frac{a^2Q^0_d}{\rho_d\mathcal{H}}\Phi'\\
&=\ -kU_d+3\mathcal{H}(C_e^2-C_a^2)\frac{\rho'_d}{\rho_d}\frac{U_d}{(1+w)k}+2\Psi\frac{a^2Q^0_d}{\rho_d}+\frac{a^2\delta Q^{0I}_d}{\rho_d}+\frac{a^2Q^{0'}_d}{\rho_d\mathcal{H}}\Phi-\frac{a^2Q^0_d}{\rho_d}\left(\frac{\Phi}{\mathcal{H}}\right)'\\
&U'_d+\mathcal{H}(1-3w)U_d=kC_e^2D_{gd}+kC_e^2\frac{\rho'_d}{\rho_d\mathcal{H}}\Phi-\left(C_e^2-C_a^2\right)\frac{U_d}{1+w}\frac{\rho'_d}{\rho_d}+(1+w)k\Psi-\frac{a^2Q^0_d}{\rho_d}U_d+(1+w)\frac{a^2\delta Q^I_{pd}}{\rho_d}
\end{aligned}
\tag{12}
$$

The quantity Φ is given by,

$$
\Phi=\frac{4\pi Ga^2\sum\rho_i\{D^i_g+3\mathcal{H}U^i/k\}}{k^2-4\pi Ga^2\sum\rho'_i/\mathcal{H}}\quad . \tag{13}
$$

To solve the above equations we have to specify the interaction form Q^ν between DE and DM. However, this is a hard task, since the nature of DE and DM remains unknown, it is not possible at the present moment to derive the precise form of the interaction between them from first principles. One has to assume a specific coupling from the outset [5, 23, 24] or determine it from phenomenological requirements [6, 19]. For the generality, we can assume the phenomenological description of the interaction between dark sectors in the comoving frame[16, 25]

$$
\begin{aligned}
Q^\nu_c&=\left[\frac{3\mathcal{H}}{a^2}(\xi_1\rho_c+\xi_2\rho_d),0,0,0\right]^T\\
Q^\nu_d&=\left[-\frac{3\mathcal{H}}{a^2}(\xi_1\rho_c+\xi_2\rho_d),0,0,0\right]^T,
\end{aligned}
\tag{14}
$$

where ξ_1,ξ_2 are small positive dimensionless constants and T is the transpose of the matrix. Choosing positive sign in the interaction, one can ensure the direction of energy transfer from DE to DM, which is required to alleviate the coincidence problem [11, 17] and avoid some unphysical problems such as negative DE density etc [15, 19]. The perturbed gauge-invariant coupling vector can be calculated by

$$
\frac{a^2\delta Q^{0I}_c}{\rho_c}=3\mathcal{H}\{\xi_1D_{gc}+\xi_2D_{gd}/r\}-3\left\{(\frac{\mathcal{H}'}{\mathcal{H}}-2\mathcal{H})(\xi_1+\xi_2/r)\right\}\Phi+\frac{a^2Q^0_c}{\rho_c}\left[\frac{\Phi}{\mathcal{H}}\right]' \tag{15}
$$

$$
\frac{a^2\delta Q^{0I}_d}{\rho_d}=-3\mathcal{H}\{\xi_1D_{gc}r+\xi_2D_{gd}\}+3\left\{(\frac{\mathcal{H}'}{\mathcal{H}}-2\mathcal{H})(\xi_1r+\xi_2)\right\}\Phi+\frac{a^2Q^0_d}{\rho_d}\left[\frac{\Phi}{\mathcal{H}}\right]' \tag{16}
$$

where $r = \rho_c/\rho_d$. For the reason as illustrated in [16, 25], we set $\delta Q^I_{pm} = \delta Q^I_{pd} = 0$. Using continuous equations to eliminate $\rho'_\lambda/\rho_\lambda$ in eq(11), eq(12), we obtain the perturbation equations[16],

$$D'_{gc} = -kU_c + 6\mathcal{H}\Psi(\xi_1 + \xi_2/r) - 3(\xi_1 + \xi_2/r)\Phi' + 3\mathcal{H}\xi_2(D_{gd} - D_{gc})/r \quad , \tag{17}$$

$$U'_c = -\mathcal{H}U_c + k\Psi - 3\mathcal{H}(\xi_1 + \xi_2/r)U_c \quad , \tag{18}$$

$$\begin{aligned} D'_{gd} = & -3\mathcal{H}C_e^2\left\{D_{gd} - 3\left(\xi_1 r + \xi_2 + 1 + w\right)\Phi\right\} - 3\mathcal{H}(C_e^2 - C_a^2)\left[\frac{3\mathcal{H}U_d}{k} - a^2 Q_d^0 \frac{U_d}{(1+w)\rho_d k}\right] \\ & -9\mathcal{H}w\left(\xi_1 r + \xi_2 + 1 + w\right)\Phi + 3\mathcal{H}wD_d + 3w'\Phi + 3(\xi_1 r + \xi_2)\Phi' - kU_d - 6\Psi\mathcal{H}(\xi_1 r + \xi_2) \\ & +3\mathcal{H}\xi_1 r(D_{gd} - D_{gc}) \end{aligned} \tag{19}$$

$$\begin{aligned} U'_d = & -\mathcal{H}(1 - 3w)U_d + kC_e^2\left\{D_{gd} - 3\left(\xi_1 r + \xi_2 + 1 + w\right)\Phi\right\} \\ & -(C_e^2 - C_a^2)a^2 Q_d^0 \frac{U_d}{(1+w)\rho_d} + 3(C_e^2 - C_a^2)\mathcal{H}U_d + (1+w)k\Psi + 3\mathcal{H}(\xi_1 r + \xi_2)U_d. \end{aligned} \tag{20}$$

In solving these equations we will adopt the adiabatic initial condition[16]

$$\frac{D_{gc}}{1 - \xi_1 - \xi_2/r} = \frac{D_{gd}}{1 + w + \xi_1 r + \xi_2}. \tag{21}$$

Dynamical stability of the DE and DM perturbations were examined in detail in [16, 25]. In the general form of the phenomenological interaction, when DE EoS $w > -1$ and we choose the coupling between dark sectors proportional to the DM energy density (by setting $\xi_2 = 0$ while keeping ξ_1 nonzero) or the total dark sectors energy density (by setting $\xi_1 = \xi_2$), we observed the dynamical instability in perturbations as argued in [15]. However, when we choose the dark sectors' mutual interaction proportional to the energy density of DE by taking $\xi_1 = 0$ and $\xi_2 \neq 0$, even for $w > -1$ we have the stable perturbations. When EoS of DE $w < -1$, no matter the interaction proportional to the energy density of the individual dark sector or the total dark sectors, the perturbation is always stable.

III. LARGE SCALE COSMIC MICROWAVE

With the formalism of the perturbation theory, we are in a position to study the CMB power spectrum. In our analysis we will concentrate on models with constant w and a constant speed of sound. The temperature anisotropy power spectrum can be calculated by

$$C_l = 4\pi \int \frac{dk}{k} \mathcal{P}_\chi(k) \mid \Delta_l(k, \tau_0) \mid^2, \tag{22}$$

where Δ_l gives the transfer function for each l, $\mathcal{P}_\chi$ is the primodial power spectrum and τ_0 is the conformal time today. On large scales the transfer functions are of the form

$$\Delta_l(k, \tau_0) = \Delta_l^{SW}(k) + \Delta_l^{ISW}(k), \tag{23}$$

where $\Delta_l^{SW}(k)$ is the contribution from the last scattering surface given by the ordinary Sachs-Wolfe (SW) effect and $\Delta_l^{ISW}(k)$ is the contribution due to the change of the gravitational potential when photons passing through the universe on their way to earth and is called the ISW effect. The ISW contribution can be written as

$$\Delta_l^{ISW} = \int_{\tau_i}^{\tau_0} d\tau j_l(k[\tau_0 - \tau]) e^{\kappa(\tau_0)-\kappa(\tau)} [\Psi' - \Phi'], \tag{24}$$

where j_l is the spherical Bessel function, κ denotes the optical depth for Thompson scattering. From Einstein equations, we obtain,

$$\Psi' - \Phi' = 2\mathcal{H}\left[\Phi + 4\pi G a^2 \sum_i U^i \rho^i/(\mathcal{H}k) + \mathcal{T}\right] - \mathcal{T}' \tag{25}$$

where

$$\Phi' = -\mathcal{H}\Phi - \mathcal{H}\mathcal{T} - 4\pi G a^2 \sum_i U^i \rho^i/k$$
$$\mathcal{T} = \frac{8\pi G a^2}{k^2}\{p^\gamma \Pi^\gamma + p^\nu \Pi^\nu\}$$

and Π is the anisotropic stress of relativistic components which can be neglected in the following discussion.

The ISW effect can be classified into early and late times effects. The early ISW effect takes place from the time following recombination to the time when radiation is no longer dynamically significant, which gives clues about what is happening in the universe from the radiation domination to matter domination. The late time ISW effect arises when DE becomes dynamically important and has the unique ability to probe the "size" of DE. When DE becomes non-negligible, the gravitational potential decays. When a photon passes throw a decaying potential well, it will have a net gain in energy and thus leads to the late ISW effect. The late ISW effect is a significant contribution to the large scale power in the temperature map of CMB.

In the minimal case when there is no interaction between DE and DM, the presence of DE perturbations leaves a w and C_e^2 dependent signature in the late ISW source term. For $w > -1$, it was observed that the CMB temperature anisotropies on large scales got enhanced for bigger constant values of C_e^2[27, 28]. It was argued that increasing C_e^2 increases the suppression of DM perturbations and therefore increases the contribution to the ISW effect[28]. However, when $w < -1$ the effect is reversed, with the perturbation initially of opposite sign, and the contribution to the ISW effect increases as the sound speed of DE is decreased[27]. The interplay between perturbations in the DE and DM and the ISW effect is very subtle and it is more direct to cross-correlate the late ISW effect to its source term, the change of the gravitational potential[27].

The late ISW effect is a promising tool to measure the EoS and sound speed of DE. Whether it can present us the signature of the interaction between DE and DM is a question we are going to address here. We will concentrate

our discussions on three commonly studied phenomenologically interaction forms between dark sectors, namely the interaction proportional to the energy density of DE, DM and total dark sectors, respectively.

When we choose the coupling between dark sectors proportional to the energy density of DE, the perturbation was found stable with an EoS $w > -1$ as well as $w < -1$[16]. For chosen constant EoS satisfying $w > -1$ and $C_e^2 = 1$, the result of large scale CMB anisotropies for different couplings are shown in Fig 1a. The lower set of dashed lines describes the late ISW effect, the middle dotted lines show the combination of the SW effect together with the early ISW effect and the top solid lines are for the total large scale CMB angular power spectra. It is clear to see that such kind of interaction between dark sectors leaves obvious signature in the late ISW effect which influences the large scale total CMB spectrum, but does not change much of the SW and early ISW effects. Comparing to the non-coupling case ($\xi_2 = 0$), the positive coupling with energy decay from DE to DM enhances the late ISW effect, while the more negative coupling with more energy decay from DM to DE suppresses more the late ISW contribution. This can be understood from the evolution of the ISW source term, the change of the gravitational potential displayed in Fig 1b. The bigger value of the coupling results in the further change of the gravitational potential. In Fig 1c we have shown the influence of the sound speed. It can be seen that the bigger sound speed of the DE makes the difference caused by different couplings bigger in the large scale CMB power spectra.

Taking constant EoS satisfying $w < -1$ and $C_e^2 = 1$, the influence of the interaction between dark sectors proportional to the energy density of DE on the large scale CMB power spectra is shown in Fig 2a. Again the coupling between dark sectors just influences the late ISW effect and thus contributes to the large scale CMB. Similar to that found in the $w > -1$ case, the late ISW contribution becomes bigger as the coupling is more positive, which is supported by the correlated potential behavior in Fig 2b. The difference in the large scale CMB power spectra induced by this kind of interaction reduces again for smaller sound speed of DE, see Fig 2c. In the case $w < -1$, we observed some irregular phenomenons when the coupling is more negative. As shown in Fig 3a, there appears a blow up behavior in the late ISW contribution for very small l and so does the very large scale total power spectra. For more negative coupling, this blow up appears because when the spatial wavenumber k becomes small enough there is a sharp increase in the potential as shown in Fig 3b. The relation between the negative coupling leading to the blow up with EoS of DE is shown in Fig 3c. Since observations suggest the deficit of large scale CMB power, thus we can rule out the too negative coupling in this interaction form.

Now we turn to discuss the coupling between dark sectors proportional to the energy density of DM, the perturbation was found stable with an EoS $w < -1$ only[16]. Choosing constant EoS with $w < -1$ and sound speed $C_e^2 = 1$, the influence of the interaction between DE and DM is displayed in Fig 4a. We see that for this kind of phenomenological

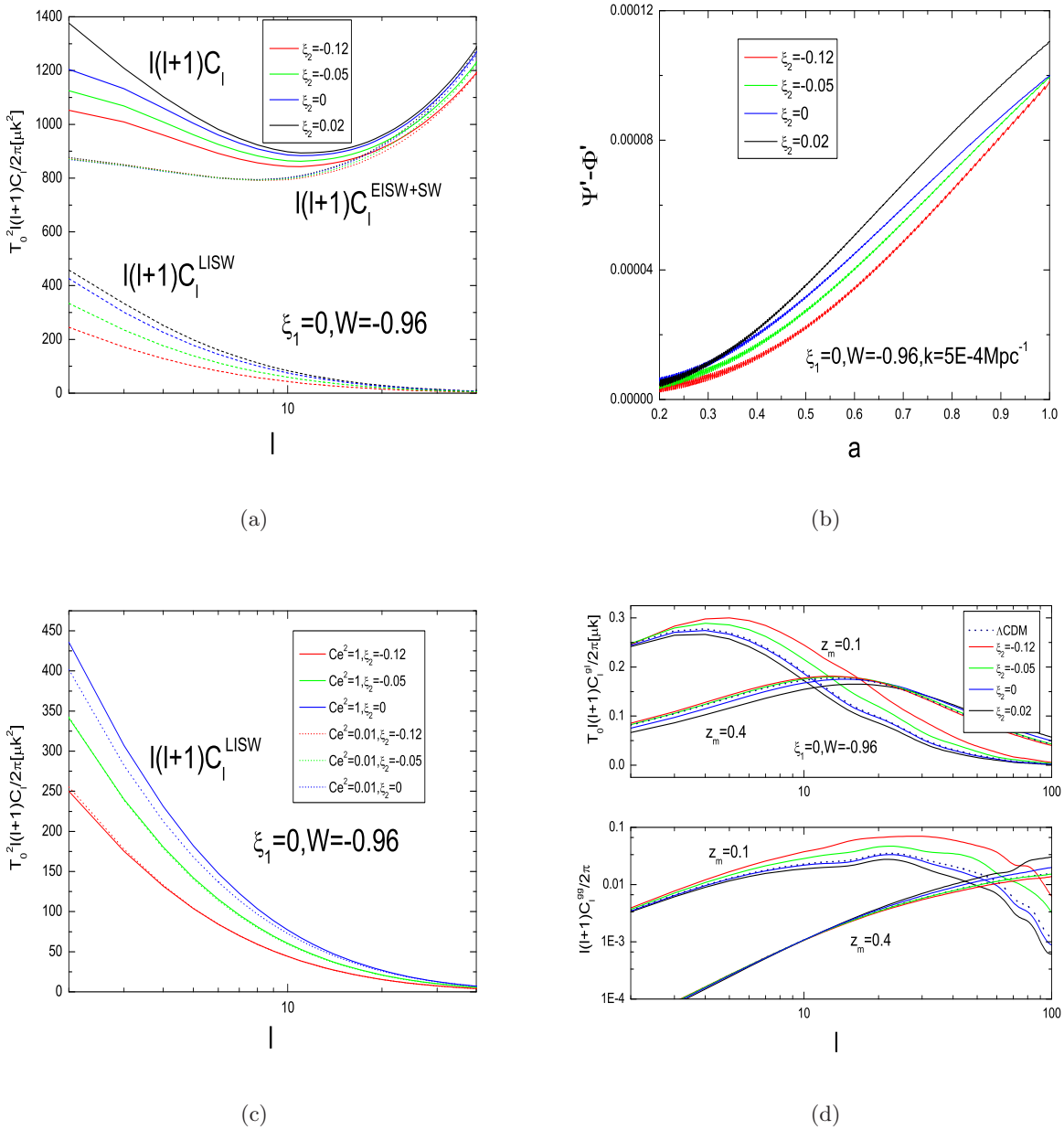

Figure 1: The small l CMB angular power spectra when the coupling is proportional to the energy density of DE. The EoS of DE satisfies $w > -1$. The up panel of (d) shows the cross-spectra and the lower panel shows the galaxy power spectra.

coupling, the SW effect together with the early ISW effect get more modification than the late ISW effect due to the coupling. Contrary to the coupling proportional to the energy density of DE case, we found that for this kind of interaction the more positive coupling results in the more suppression in the CMB anisotropies. This is reasonable if we look at its correlated potential behavior, see Fig 4b. In Fig 4c we have shown that the smaller sound speed of DE will enhance the difference in the very large scale power in the temperature map, which is also different from the

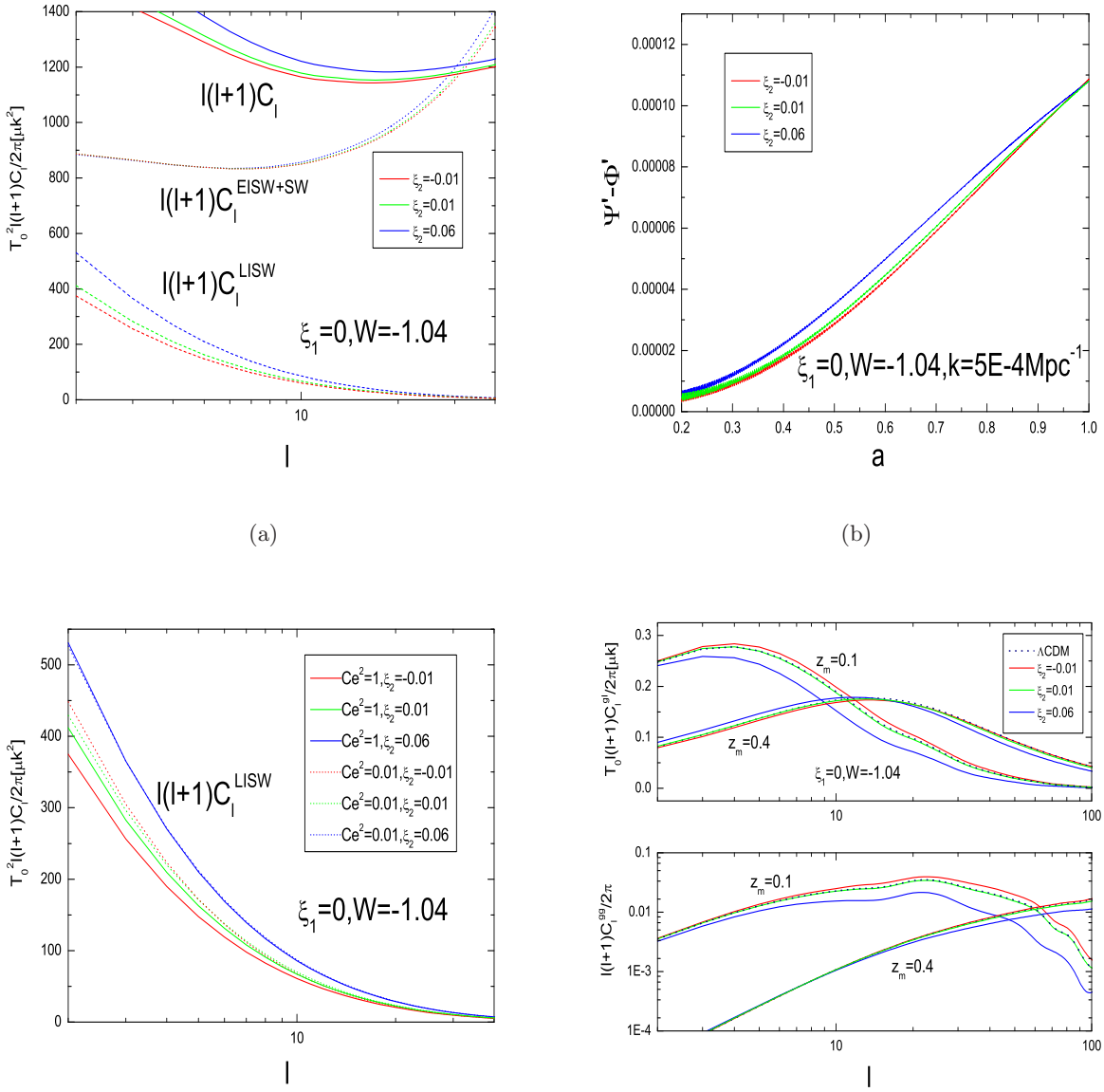

Figure 2: The small l CMB angular power spectra when the coupling is proportional to the energy density of DE. The EoS of DE satisfies $w < -1$.The up panel of (d) shows the cross-spectra and the lower panel shows the galaxy power spectra.

result we have seen above for the coupling proportional to the DE energy density.

For the interaction between DE and DM proportional to the energy density of total dark sectors, we list our results in Fig 5, which is very similar to that we observed when the interaction proportional to the energy density of DM.

With the formalism of the perturbation theory when DE and DM are in interaction, we have analyzed the signature of the coupling between dark sectors from the large scale CMB anisotropies. The large scale power in the temperature

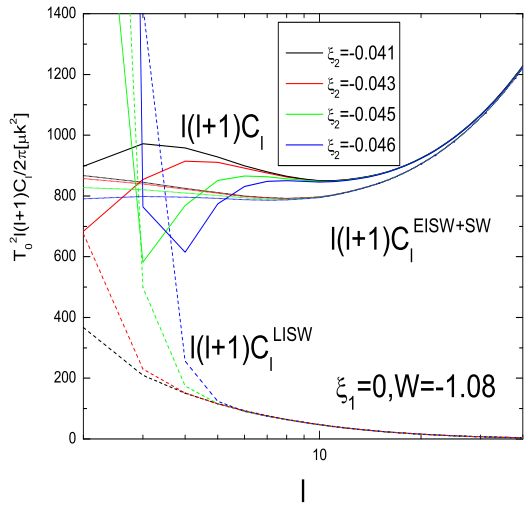

(a)

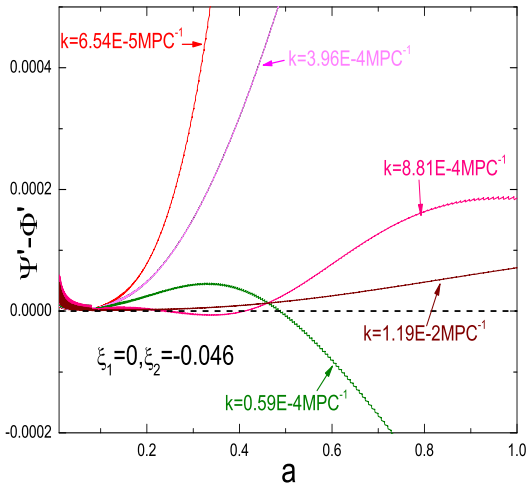

(b)

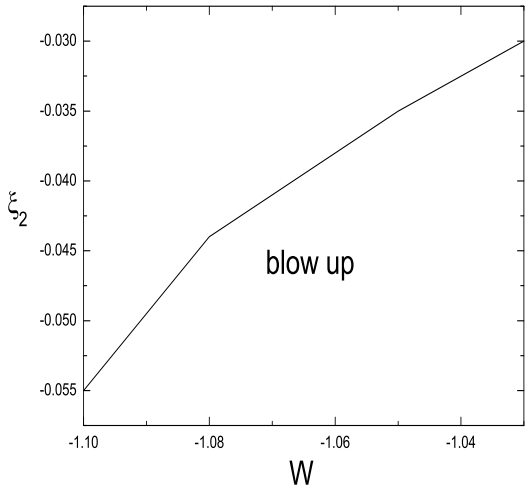

(c)

Figure 3: The irregular behaviors of the small l angular power spectra when the couplings get too negative. Figure (c) indicates the blow up with regard to ξ_2 and w.

map looks very different when interactions are included and this provides the possibilities to use the large scale CMB information to constrain the coupling between dark sectors.

By far we only discuss the influence of the ISW effect on the CMB auto power spectrum. Since the late ISW effect arises from the time varying gravitational potential, which correlates with the large scale structure (LSS) of the universe, the cross correlating CMB with tracers of LSS provides another way of measuring the ISW effect [37].

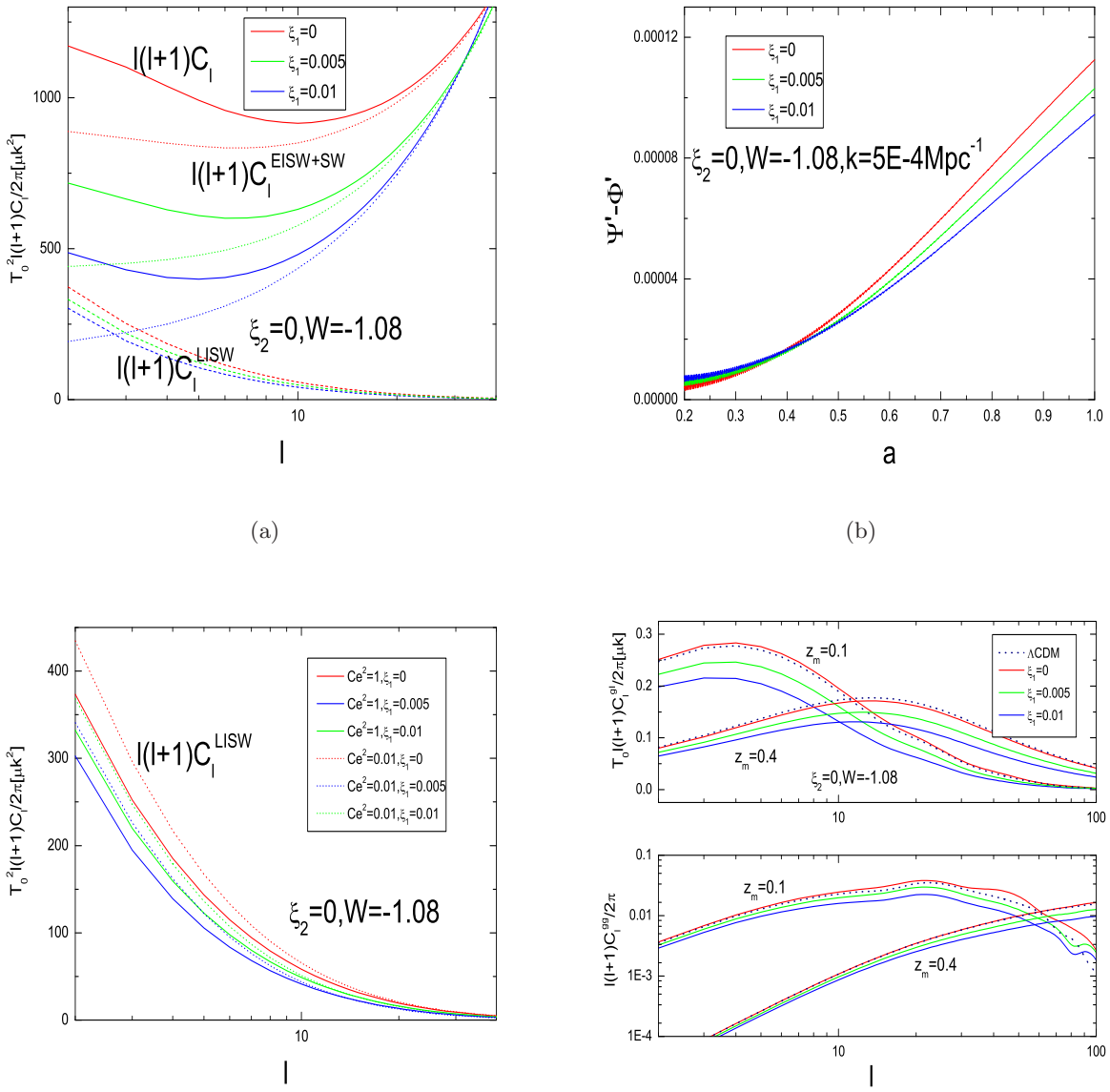

Figure 4: The small l CMB angular power spectra when the coupling is proportional to the energy density of DM. The DE EoS satisfies $w < -1$. The up panel of (d) shows the cross-spectra and the lower panel shows the galaxy power spectra.

Progresses in CMB and LSS surveys have enabled detections of the ISW-LSS cross correlation at $\sim 3\sigma$ level [38]. The S/N can be further improved by a factor of a few for future all sky LSS surveys. This cross correlation technique has a number of advantages. First, the primary CMB does not correlate with the LSS and thus does not bias the ISW measurement. Second, the cross correlation signal is $\propto \Delta T_{\rm ISW}$, which tells whether the potential decays or grows. The later case can happen in our interacting dark matter-dark energy models (e.g, panel b, Fig. 3) and in modified gravity

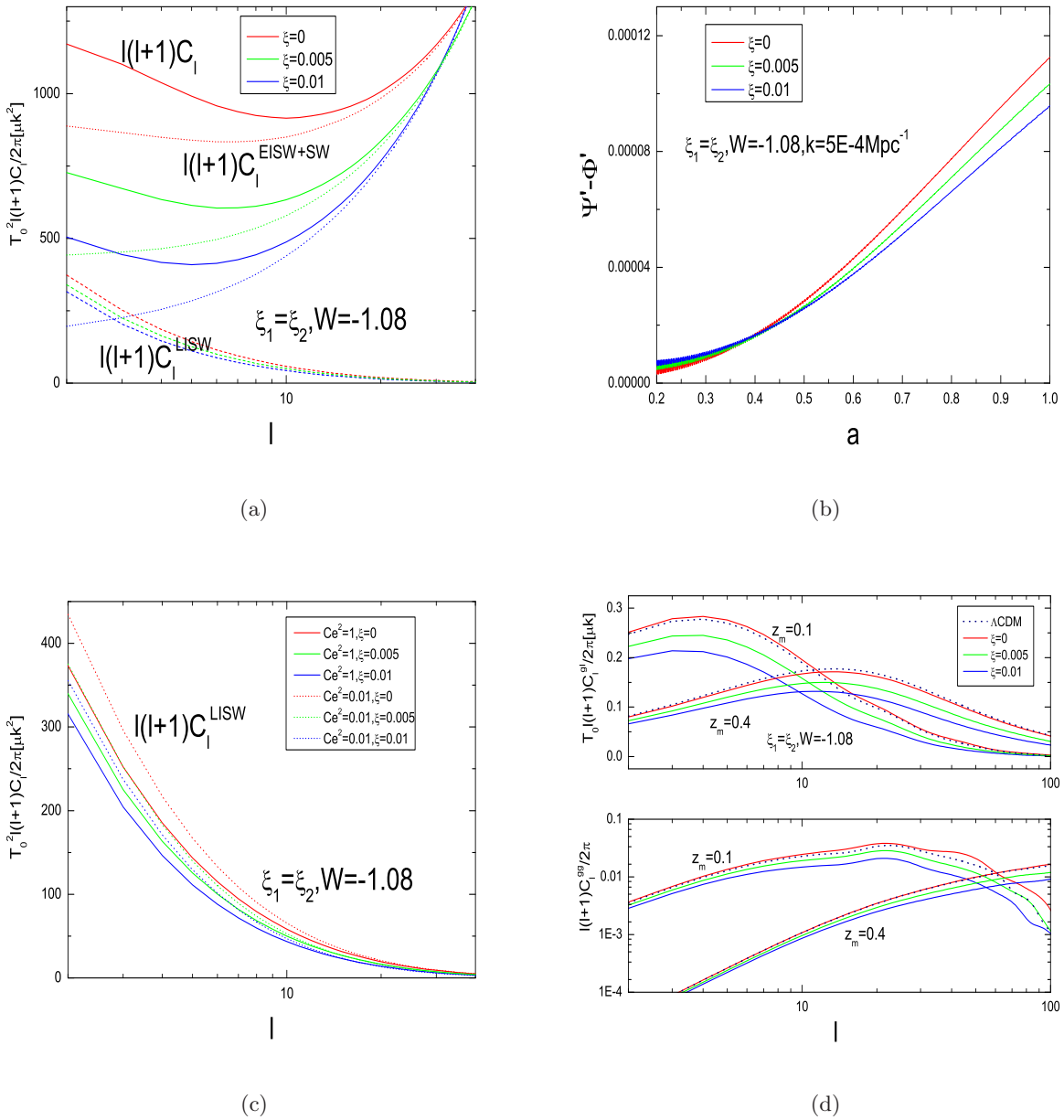

Figure 5: The small l CMB angular power spectra when the coupling is proportional to the energy density of total dark sectors and the EoS $w < -1$.The up panel of (d) shows the cross-spectra and the lower panel shows the galaxy power spectra.

models. As a comparison, the CMB auto power spectrum is only sensitive to $\Delta T^2_{\rm ISW}$ and thus loses this capability. Third, through the redshift distribution of the LSS, we are able to recover the redshift evolution of the gravitational potential and thus infer more details on the dark matter-dark energy interaction. Thus the ISW-LSS cross correlation is potentially powerful for probing the dark matter-dark energy interaction. However, due to the low signal-to-noise ratio of the current ISW-LSS measurements and the complexities in the theoretical interpretation (e.g. the galaxy

bias), we will not confront our model predictions against the existing ISW-LSS cross correlation measurement in this paper. Instead, we will just calculate the expected cross correlation signal between the ISW effect and galaxies, for some representive cases.

The auto- and cross-correlation power spectra are given by

$$C_l^{gg} = 4\pi \int \frac{dk}{k} \mathcal{P}_\chi(k) I_l^{g*}(k) I_l^g(k) \tag{26}$$

$$C_l^{gI} = 4\pi \int \frac{dk}{k} \mathcal{P}_\chi(k) I_l^{g*}(k) \Delta_l^{ISW}(k), \tag{27}$$

where the integrand for galaxy densities $I_l^g(k)$ reads,

$$I_l^g(k) = \int dz b_g(z) \Pi(z) (D_{gc} + D_{gb}) j_l[k\chi(z)]. \tag{28}$$

Here $b_g(z)$ is the galaxy bias, $\Pi(z)$is the redshift distribution and $\chi(z)$ is the conformal distance, or equivalently the look-back time from the observer at redshift $z = 0$,

$$\chi(z) = \int_0^z \frac{dz'}{H(z)} = \int_{\tau_i(z)}^{\tau_0} d\tau = \tau_0 - \tau_i(z). \tag{29}$$

We assume $b(z) \sim 1$ for simplicity and adopt the redshift distribution of the form[39],

$$\Pi(z) = \frac{3}{2} \frac{z^2}{z_0^3} \exp\left[-(\frac{z}{z_0})^{3/2}\right] \tag{30}$$

normalized to unity and peaking near the median redshift $z_m = 1.4 z_0$. For illustrative purpose,we choose $z_m = 0.1$ and $z_m = 0.4$ throughout our analysis. The first choice resembles a shallow survey like 2MASS and the second one resembles a survey similar to SDSS photo-z galaxy samples.

When the coupling is proportional to the energy density of DE and the EoS is larger than $-1 (w > -1)$, the cross power spectra and auto correlation power spectra of galaxies are shown in Fig 1d. For lower redshift galaxies survey $z_m = 0.1$, comparing with the LCDM model we see that the couplings significantly change both the cross spectra and the auto spectra. The negative couplings enhance the power of the correlation while the positive couplings hinder such correlation. When the EoS is smaller than -1, we find very similar results as shown in Fig 2d. However, for deeper redshift galaxies survey $z_m = 0.4$, the couplings do not imprint significantly on the cross power spectra and auto correlation power spectra of galaxies as compared with $z_m = 0.1$.

When the coupling is proportional to the energy density of DM or total dark sectors, we find from Fig 4d,Fig 5d that the cross power spectra are more sensitive to the couplings at lower l part than that of higher l part when the median redshift around 0.1. This feature is different from that shown in Fig 1d and Fig 2d when the interaction is proportional to the energy density of DE, where it was found that at small l when ISW effect amplified, the ISW-LSS

cross-correlation is not so much different due to the coupling. While in the other way, for higher redshift survey $z_m = 0.4$, we find less such effect on the cross and auto spectra.

The qualitative behaviors presented here show that the 2MASS survey has more possibility in discriminating the interaction between dark sectors than that of SDSS survey. It is expected in the future that galaxy surveys with photo-z measurements or even spec-z measurements, along with better CMB measurements, could provide better ISW-LSS cross-correlation measurements at each redshift bin. However, since the latest result on the measurement of this effect is not better than $\sim 3\sigma$ [40] in accuracy, we will not incorporate the relevant data set in our global fitting in this work.

In the next section we are going to report the fitting result by comparing with observations of CMB.

IV. CONSTRAINTS USING OBSERVATIONAL DATA AND THE COINCIDENCE PROBLEM

In order to further see the signature of the interaction between DE and DM, in this section we will compare our model with observational data by using joint likelihood analysis. We take the parameter space as

$$P = (h, \omega_b, \omega_{cdm}, \tau, \ln[10^{10} A_s], n_s, \xi_1, \xi_2, w)$$

where h is the hubble constant, $\omega_b = \Omega_b h^2, \omega_{cdm} = \Omega_{cdm} h^2$, A_s is the amplitude of the primordial curvature perturbation, n_s is the scalar spectral index, ξ_1 and ξ_2 are coupling constants proportional to the energy density of DM and DE respectively, w is the EoS of DE. We choose the flat universe with $\Omega_k = 0$ and our work is based on CMBEASY code[29].

In the global fitting, we have used CMB data coming from WMAP5 temperature and polarization power spectra. We used Gibbs sampling routine provided by WMAP team for the likelihood calculation. In the small scale CMB measurements, we included BOOMERanG[30], CBI [31], VSA[32] and ACBAR[33] data. In order to get better constraint on the background evolution, we have added SNIa[34] data and marginalized over the nuisance parameters. We also incorporated the data from large scale luminous red galaxies(LRGs) survey, we used SDSS[35] data as powerful constraint on real-space power spectrum $P(k)$ at redshift $z \sim 0.1$.

Since the terms incorporating Q_d^0 on the left hand sides of eq.(19,20) encounter the irreducible singularity when w crossing -1, we therefore set prior on EoS either $w > -1$ or $w < -1$. We take the effective sound speed $C_e^2 = 1$ in our analysis.

The global fitting results for different forms of interaction between dark sectors are shown below:

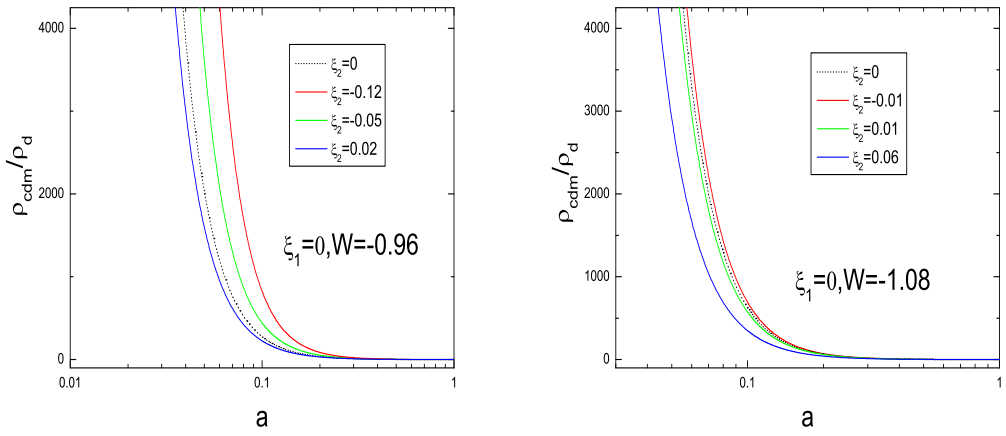

Figure 6: The behaviors of the ratio $r = \rho_c/\rho_d$ when the coupling is proportional to the energy density of DE. The left one for $w > -1$ and the right one for $w < -1$.

A. The interaction proportional to DE energy density

For the DE EoS $w > -1$, we have the result

h	$\Omega_b h^2$	$\Omega_{cdm} h^2$	τ	$\ln[10^{10} A_s]$	n_s	$\xi_1 = 0, \xi_2 \neq 0$	$1 + w > 0$
$0.687^{+0.013}_{-0.013}$	$0.0225^{+0.0006}_{-0.0005}$	$0.107^{+0.007}_{-0.009}$	$0.091^{+0.017}_{-0.016}$	$3.109^{+0.033}_{-0.031}$	$0.963^{+0.013}_{-0.013}$	$-0.028^{+0.023}_{-0.032}$	< 0.052

For the phantom DE EoS $w < -1$,we constrain $\xi_2 > 0.030$ to avoid the blow-up and we have

h	$\Omega_b h^2$	$\Omega_{cdm} h^2$	τ	$\ln[10^{10} A_s]$	n_s	$\xi_1 = 0, \xi_2 \neq 0$	$1 + w < 0$
$0.700^{+0.012}_{-0.011}$	$0.0223^{+0.0006}_{-0.0005}$	$0.119^{+0.009}_{-0.006}$	$0.086^{+0.019}_{-0.016}$	$3.105^{+0.033}_{-0.032}$	$0.956^{+0.013}_{-0.014}$	$-0.010^{+0.025}_{-0.020}$	$-0.051^{+0.051}_{-0.043}$

In both cases we observed from the global fitting that the coupling between DE and DM in the 1σ range can either be positive or negative. Using the best-fit results, we have studied the coincidence problem. We paid attention to the ratio of energy densities between DE and DM, $r = \rho_c/\rho_d$, and its evolution. No matter for $w > -1$ or $w < -1$, we observed that a slower change of r for positive coupling as compared to the noninteracting case. This means that the period when energy densities of DE and DM are comparable is longer when there is a positive coupling between DE and DM, see Fig 6 for an example.

B. The interaction proportional to DM energy density

Now we report the fitting result for the interaction between dark sectors proportional to the energy density of DM.

h	$\Omega_b h^2$	$\Omega_{cdm} h^2$	τ	$\ln[10^{10} A_s]$	n_s	$\xi_1 > 0, \xi_2 = 0$	$1 + w < 0$
$0.690^{+0.015}_{-0.015}$	$0.0224^{+0.0005}_{-0.0005}$	$0.121^{+0.003}_{-0.003}$	$0.094^{+0.016}_{-0.017}$	$3.115^{+0.034}_{-0.033}$	$0.953^{+0.013}_{-0.013}$	$0.0007^{+0.0006}_{-0.0006}$	$-0.072^{+0.072}_{-0.053}$

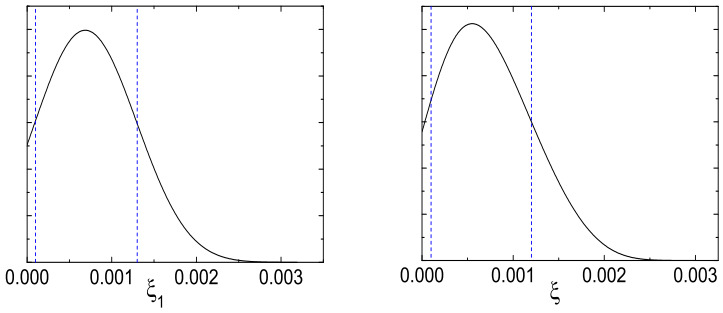

(a) (b)

Figure 7: The likelihood for the coupling constant when the interaction is proportionl to the energy density of DM (left) and the total dark sectors (right).

It is interesting to see that for this kind of interaction, the global fitting told us that in 1σ range the coupling between DE and DM is always positive, see Fig 7a. This is encouraging, since for positive coupling with the energy decay from DE to DM we can always have the slower change of r as compared to the noninteracting case as shown in Fig 8. Thus with this kind of interaction the coincidence problem can be overcome. Another interesting point is that employing this kind of interaction form we can constrain the coupling to a very precise value compared with the interaction proportional to the energy density of DE. This is because this kind of interaction shows up not only in the late ISW effect, but also the SW and early ISW effects as shown in Fig 4. As displayed in Fig 8, DE and DM can trace each other from very early period. It can leave imprints in at smaller scales (bigger l multipoles) where there are more independnet modes to improve observation accuracy. This can help to reduce the uncertainty in determining the coupling constant for this kind of interaction.

C. The interaction proportional to energy density of total dark sectors

For the interaction proportional to the energy density of total dark sectors, we have obtained the similar result as in the above subsection. The results are shown below:

h	$\Omega_b h^2$	$\Omega_{cdm} h^2$	τ	$\ln[10^{10} A_s]$	n_s	$\xi = \xi_1 = \xi_2 > 0$	$1 + w < 0$
$0.690^{+0.014}_{-0.014}$	$0.0224^{+0.0006}_{-0.0006}$	$0.121^{+0.004}_{-0.003}$	$0.093^{+0.018}_{-0.017}$	$3.114^{+0.036}_{-0.033}$	$0.955^{+0.014}_{-0.014}$	$0.0006^{+0.0006}_{-0.0005}$	$-0.065^{+0.065}_{-0.054}$

The likelihood of the coupling constant is shown in Fig 7b. The evolution of the ratio of energy densities between DE and DM for this kind of interaction is shown in Fig 9.

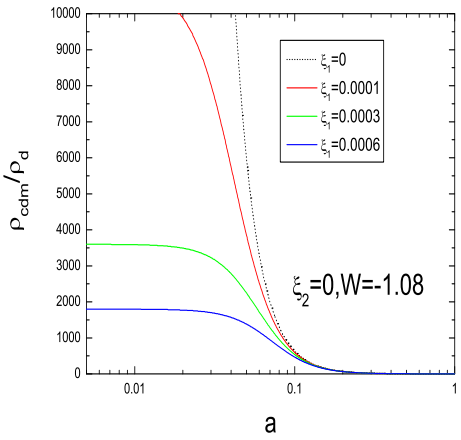

Figure 8: The behaviors of the ratio $r = \rho_{cdm}/\rho_d$ when the coupling is proportional to the energy density of DM.

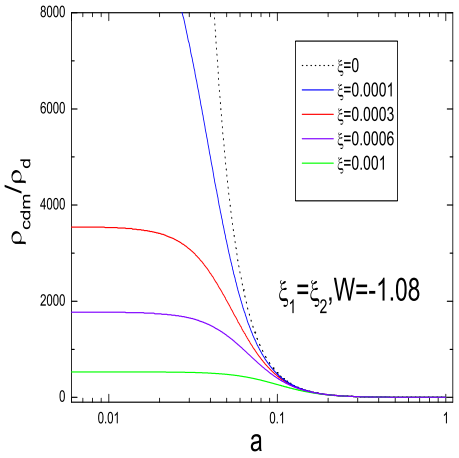

Figure 9: The behaviors of the ratio $r = \rho_{cdm}/\rho_d$ when the coupling is proportional to the energy density of total dark sectors.

V. CONCLUSIONS AND DISCUSSIONS

We have reviewed the formalism of the perturbation theory when there is interaction between DE and DM. Based upon this formalism we have studied the signature of the interaction between dark sectors in the CMB large scale temperature fluctuations. We found that in addition to disclose the DE EoS, sound speed, the late ISW effect is a promising tool to measure the coupling between dark sectors. When the interaction between DE and DM takes the form proportional to the energy density of DM and the total dark sectors, because in these cases DE and DM started to chase each other since early time, the interaction not only presents in the late ISW source term but also leaves imprint in the SW and early ISW effects. These properties provide a possible way to examine the interaction between

DE and DM even from smaller scale in CMB observations.

We have performed the global fitting by using the CMB power spectrum data including WMAP5 data and balloon observational data together with SNIa and SDSS data to constrain the interaction between DE and DM. When the interaction between DE and DM takes the form proportional to the energy density of DM and the total dark sectors, since it leaves more information in the CMB power spectra, not only just in the very large scale, the coupling can be constrained in a very precise range. In 1σ the coupling is positive indicating that there is energy transfer from DE to DM. This kind of energy transfer can help to alleviate the coincidence problem compared to the noninteracting case.

It is of great interest to extend our study to a field theory description of the interaction between DE and DM and examine its signature in the large scale CMB power spectra. A possible field theory model was proposed in [36] and further investigation in this direction is called for.

Acknowledgments

This work has been supported partially by NNSF of China, Shanghai Science and Technology Commission and Shanghai Education Commission. We would like to acknowledge helpful discussions with X. L. Chen, Y. G. Gong, F. Q. Wu and the hospitality of KITPC where main part of the work was carried out.

[1] S. J. Perlmutter et al., Nature 391, 51 (1998); A. G. Riess et al., Astron. J. 116, 1009 (1998); S. J. Perlmutter et al., Astroph. J. 517, 565 (1999); J. L. Tonry et al., Astroph. J. 594, 1, (2003); A. G. Riess et al., Astroph. J. 607, 665 (2005); P. Astier et al., Astron. Astroph. 447, 31 (2005); A G. Riess et al., Astroph. J. 659, 98 (2007).
[2] M. Kowalski et al., 2008, arXiv:0804.4142.
[3] M. Tegmark et al., Phys. Rev. D 74, 123507 (2006).
[4] L. Amendola, Phys. Rev. D 62, 043511 (2000); L. Amendola and C. Quercellini, Phys. Rev. D 68, 023514 (2003); L. Amendola, S. Tsujikawa and M. Sami, Phys. Lett. B 632, 155 (2006).
[5] D. Pavon, W. Zimdahl, Phys. Lett. B 628, 206 (2005), S. Campo, R. Herrera, D. Pavon, Phys. Rev.D 78, 021302(R) (2008).
[6] G. Olivares, F. Atrio-Barandela and D. Pavon, Phys. Rev. D 74, 043521 (2006).
[7] C. G. Boehmer, G. Caldera-Cabral, R. Lazkoz, R. Maartens, Phys. Rev. D 78, 023505 (2008).
[8] S. B. Chen, B. Wang, J. L. Jing, Phys.Rev.D 78, 123503 (2008).
[9] B. Wang, J. Zang, C.-Y. Lin, E. Abdalla and S. Micheletti, Nucl. Phys. B 778, 69 (2007).
[10] W. Zimdahl, Int. J. Mod. Phys. D 14, 2319 (2005).
[11] D. Pavon, B. Wang, Gen. Relav. Grav. (in press), arXiv:0712.0565.
[12] B. Wang, C.-Y. Lin, D. Pavon, E. Abdalla, Phys. Lett. B 662, 1, (2008).
[13] O. Bertolami, F. Gil Pedro and M. Le Delliou, Phys. Lett. B 654, 165 (2007). O. Bertolami, F. Gil Pedro and M. Le Delliou, arXiv:0705.3118v1.
[14] Z. K. Guo, N. Ohta and S. Tsujikawa, Phys. Rev. D 76, 023508 (2007).
[15] J. Valiviita, E. Majerotto, R. Maartens, JCAP 07, 020 (2008), ArXiv:0804.0232.
[16] J. H. He, B. Wang, E. Abdalla, Phys. Lett. B 671, 139 (2009), ArXiv:0807.3471
[17] W. Zimdahl, D. Pavon, L.P. Chimento, Phys. Lett. B 521, 133 (2001); L.P. Chimento, A.S. Jakubi, D. Pavon, W. Zimdahl, Phys. Rev. D 67, 083513 (2003).
[18] E. Abdalla, L.Raul W. Abramo, L. Sodre Jr., B. Wang, Phys. Lett. B673, 107 (2009) ArXiv:astro-ph/0710.1198.
[19] J. H. He, B. Wang, JCAP 06, 010 (2008), ArXiv:0801.4233.
[20] C. Feng, B. Wang, E. Abdalla, R. K. Su, Phys. Lett. B 665, 111 (2008), arXiv:0804.0110.
[21] B. Jackson, A. Taylor, A. Berera, arXiv:0901.3272.
[22] A. Refrefier, et al, ArXiv: 0802.2522.
[23] S. Das, P. S. Corasaniti and J. Khoury, Phys. Rev. D 73, 083509 (2006).

[24] L. Amendola, D. Tocchini-Valentini, Phys. Rev. D64, 043509 (2001); G. W. Anderson, S. M. Carroll, ArXiv:astro-ph/9711288.
[25] J. H. He, B. Wang, Y. P. Jing, JCAP 07, 030 (2009) ArXiv:0902.0660.
[26] G. Caldera-Cabral, R. Maartens, B. Schaefer, arXiv:0905.0492.
[27] J. Weller, A. M. Lewis, Mon. Not. Roy. Astron. Soc. 346, 987 (2003), ArXiv:astro-ph/0307104.
[28] R. Bean, O. Dore, Phys.Rev. D 69, 083503 (2004),ArXiv:astro-ph/0307100.
[29] M. Doran, JCAP 0510, 011 (2005).
[30] C. J. MacTavish, et al., Astrophys. J. 647, 799 (2006).
[31] A. C. S. Readhead, et al., Astrophys. J. 609, 498 (2004).
[32] C. Dickinson, et al., Mon. Not. Roy. Astron. Soc. 353, 732 (2004).
[33] C. L. Reichardt, et al., ArXiv:0801.1491.
[34] A. G. Riess, et al., ArXiv:astro-ph/0611572.
[35] P. McDonald, et al., Astrophys. J. Suppl. 163, 80(2006); P. McDonald, et al., Astrophys. J. 635, 761 (2005).
[36] S. Micheletti, E. Abdalla, B. Wang, Phys. Rev. D (in press) ArXiv:0902.0318.
[37] Robert G. Crittenden, Neil Turok, Phys.Rev.Lett. 76 (1996) 575; Uros Seljak, Matias Zaldarriaga, Phys.Rev. D60 (1999) 043504; A. Cooray, Phys. Rev. D 65, 103510 (2002)
[38] S. Boughn, R. Crittenden, Nature 427 (2004) 45-47; M.R. Nolta, et al., Astrophys.J. 608 (2004) 10-15; P. Fosalba, E. Gaztanaga, Mon.Not.Roy.Astron.Soc. 350 (2004) L37-L41; P. Fosalba, et al., Astrophys.J. 597 (2003) L89-92; R. Scranton, et al. 2003, astro-ph/0307335; P. Vielva, E. Martinez-Gonzalez, M. Tucci, astro-ph/0408252; N. Afshordi, Y.S. Loh, M. Strauss, Phys.Rev. D69 (2004) 083524; Nikhil Padmanabhan, et al. Phys.Rev. D72 (2005) 043525; A. Cabre, et al., MNRAS 381, 1347 (2007); G. Olivares, et al., Phys. Rev. D 77 103520 (2008); B. M. Schaefer, MNRAS 388, 1403 (2008).
[39] J. Lesgourgues, W. Valkenburg, E. Gaztanaga, Phys, Rev. D77 063505 (2008).
[40] T. Giannantonio, et al., Phys. Rev. D77, 123520 (2008); S. Ho, et al., Phys. Rev. D 78 043519 (2008).